Available online at www.sciencedirect.com

ScienceDirect

journal homepage: www.elsevier.com/locate/he

Optimal integration modeling of Co – Electrolysis in a power-to-liquid industrial process

José Sánchez-Luján [a], Ángel Molina-García [b,*], José Javier López-Cascales [a]

[a] Department of Chemical and Environmental Engineering. Universidad Politécnica de Cartagena, 30203 Cartagena Spain

[b] Department of Automatics, Electrical Engineering and Electronic Technology, Universidad Politécnica de Cartagena, 30202 Cartagena Spain

HIGHLIGHTS

- Novel Green Syngas technology integration into industrial scale plants.
- Overall Plant efficiency 76% HHV.
- Plant Flexible design for continuous full FT synthesis capacity operation.
- Basis for utilization in the CPOX the Oxygen produced by SOEC.

GRAPHICAL ABSTRACT

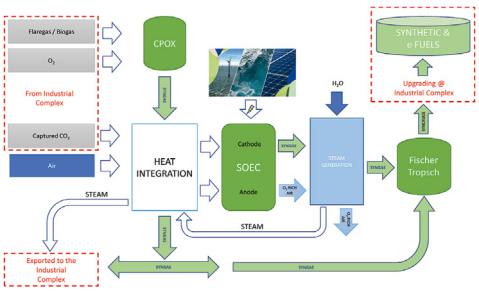

ARTICLE INFO

Article history:
Received 29 December 2022
Received in revised form
30 June 2023
Accepted 2 July 2023
Available online xxx

Keywords:
Solid-oxide co-electrolysis
Green syngas
Power to liquid
Fischer tropsch
Catalytic partial oxidation

ABSTRACT

High temperature co-electrolysis using solid-oxide electrolysis cells is a highly efficient pathway for green syngas production owing to the possibility of heat integration with other processes. Therefore, this study described and evaluates a flexible and efficient configuration for producing sustainable synthetic fuels using electricity from renewables and captured CO_2 by integrating co-electrolysis in a power-to-liquid industrial plant. Thereafter, novel and efficient technologies were implemented for green syngas production and its subsequent purification, increasing the overall process efficiency and achieving a significant reduction in the carbon footprint compared to mature synthetic crude production processes. Catalytic partial oxidation and dual pressure swing adsorption were integrated with co-electrolysis and Fischer–Tropsch synthesis in a scaled industrial plant, using residual streams from the complex or those of renewable origin as feed, which allowed the continuous operation of the process independent of renewable power generation. The mass and energy balance, performance, and efficiency estimations were also included in this study. A solid-oxide electrolytic cell (SOEC) plant using renewable electricity and heat input from thermal integration with the outlet syngas stream of the catalytic partial oxidation reactor was selected as a case study. Both the performance and efficiency analyses of the co-electrolysis unit demonstrated the benefits of such thermal integration in comparison with current solutions. In this study, both the thermal integration of the

* *Corresponding author.*
E-mail address: angel.molina@upct.es (Á. Molina-García).

https://doi.org/10.1016/j.ijhydene.2023.07.012

0360-3199/© 2023 The Author(s). Published by Elsevier Ltd on behalf of Hydrogen Energy Publications LLC. This is an open access article under the CC BY-NC-ND license (http://creativecommons.org/licenses/by-nc-nd/4.0/).

Please cite this article as: Sánchez-Luján J et al., Optimal integration modeling of Co – Electrolysis in a power-to-liquid industrial process, International Journal of Hydrogen Energy, https://doi.org/10.1016/j.ijhydene.2023.07.012

process streams, as well as the energy and heat consumed by the syngas purification process were considered.

© 2023 The Author(s). Published by Elsevier Ltd on behalf of Hydrogen Energy Publications LLC. This is an open access article under the CC BY-NC-ND license (http://creativecommons.org/licenses/by-nc-nd/4.0/).

Introduction

The awareness created in society regarding environmental responsibility and sustainable development has triggered the articulation of policies necessary to achieve the zero-emissions objective. In line with the milestone horizons of sustainability by 2030 [1] and decarbonization by 2050, different initiatives have been promoted to replace fossil fuels, fundamentally transitioning toward a hydrogen-based economy [2]. Owing to the remarkable integration of renewable energy sources into power systems, the development of green hydrogen production technologies, including electrolysis, has been widely proposed, allowing the production of hydrogen without an associated carbon footprint [3]. Subsequently, and according to recent reports, the total hydrogen global demand has rapidly increased from 255.3 billion m3 in 2013 to 324.8 billion m3 in 2020. Hydrogen is required in most petrochemical processes, and Steam Methane Reforming (SMR) is the most widely used technology adopted for hydrogen generation [4]. Wang et al. [5] affirmed that hydrogen, as a secondary energy source, should be extracted from other substances, such as water and hydrocarbons, through energy conversion processes such as water electrolysis and thermochemistry. Because solar irradiation and wind cannot be controlled, some researchers have proposed the use of excess electric energy produced by renewable power plants during periods of low demand to produce synthetic fuels [6], including hydrogen, methane, methanol, dimethyl ether, or synthetic Diesel [7]. Nevertheless, synthetic fuels have some advantages over hydrogen, mainly in terms of avoiding significant changes to the current facilities. They can be used with current infrastructure and vehicles [8]. Therefore, in the current energy transition, synthetic fuels must play a key role, particularly in sectors that are difficult to electrify and those where the implantation of green hydrogen requires the development of alternative technologies.

Among the various solutions, co-electrolysis is considered as one of the most promising emerging technologies for integration into synthetic fuel production processes. It is based on CO_2 captured by different carbon capture technologies developed for industrial decarbonization processes. Energy generation and hydrocarbon production through synthesis gas (syngas) have been investigated for decades as alternatives to liquid fossil fuels [9]. Co-electrolysis of CO_2 and water can provide a cost-effective alternative to mature technologies for converting electricity into syngas [10]. Syngas is a gaseous mixture that is used as the starting material for petrochemicals and fuels. It was composed of different ratios of carbon monoxide (CO) and hydrogen (H2) in different ratios [11]. The syngas required for the synthesis of synthetic crude oil can be obtained using different methods: (i) water electrolysis and reverse water–gas shift (rWGS) [4], (ii) water electrolysis and carbon dioxide electrolysis [12], and (iii) co-electrolysis. In this study, co-electrolysis was selected as the syngas production pathway for liquid fuel synthesis. The Fischer–Tropsch (FT) reaction has been reported for the synthesis of hydrocarbons and other organic compounds [13]. The FT synthesis is an important technology for converting syngas into liquid synthetic fuels. The FT usually requires a complex product upgrading section [14]. Existing conventional routes utilize natural gas or coal as feedstock for syngas generation. These technologies are known as gas-to-liquid (GtL) and coal-to-liquid (CtL) technologies [15].

Several studies have focused on the production of syngas via co-electrolysis to produce synthetic fuels. Becker et al. [16] developed a high temperature co-electrolysis (HTCE) model based on carbon dioxide and water. They used solid-oxide electrolytic cells (SOEC) for syngas production and the FT reaction for liquid fuel conversion. The effects of various parameters such as temperature, pressure, and feedstock composition on the syngas outlet composition exiting the SOEC were analyzed. The overall system efficiency for liquid hydrocarbon fuels produced from electrical energy was 54.8% HHV (51.0%LHV). It was determined that operating the SOEC at a low pressure versus high pressure resulted in an efficiency gain of 2.6%. The economics of the production plant were also evaluated, focusing on variations in the electricity feedstock costs and operating capacity factors. The purification processes for the syngas and side coke formation reactions were not considered in this study. Herz G. et al. [17] introduced power-to-liquid (PtL) processes as a key technology for fossil-free raw materials and energy systems. Technical feasibility analyses were performed and subsequently tested using the pilot plants. The influence of the operating conditions of the solid-oxide electrolyzer on the process economics and optimization is also discussed. Tremel A. et al. [18] proposed hydrogen production from renewables via water electrolysis coupled with downstream chemical synthesis. Current facilities can be used directly for liquid fuel production, avoiding any modifications to be included in a 100% green hydrogen scenario. Various one-stage synthesis systems have been evaluated in terms of technology and economics. König D. H et al. [19] proposed a model concept based on H_2 from electrolysis, reacting with CO_2 in a reverse water–gas shift reactor. The syngas was then synthesized in an FT reactor. The reported PtL efficiency was 43.3% and the carbon conversion rate was 73.7%. Wang L. et al. [20] introduced the concept of power-to-X systems via solid-oxide electrolysis as a promising technology for storing excess renewable electricity via efficient co-electrolysis. Syngas can then be

Please cite this article as: Sánchez-Luján J et al., Optimal integration modeling of Co – Electrolysis in a power-to-liquid industrial process, International Journal of Hydrogen Energy, https://doi.org/10.1016/j.ijhydene.2023.07.012

converted into synthetic fuel via plane-wise thermal integration. A quasi-2D model was calibrated using data from 6000 h of stack testing under laboratory isothermal conditions. The results showed that the production system efficiency of H_2, methane, methanol/dimethyl ether, and gasoline decreased sequentially from 94% (power-to-H_2) to 64% (power-to-gasoline), based on a higher heating value. Co-electrolysis is suitable for improving the efficiency of systems with fewer exothermic fuel synthesis processes and allows for better heat integration. Recently, Wang F. et al. [21] integrated a diesel engine with SOEC stacks as heat recovery steam generators (HRSG). An SOEC plant that used electricity as the thermal heat input was selected as a case study. Thermodynamic analysis of the benchmark and integration schemes estimated that electrical efficiencies of 73.12% and 85.17% could be achieved, respectively. The diesel-to-power efficiency increased to 70% when the exhaust gas was completely utilized by the SOEC system. Water electrolysis based on SOEC exhibits relevant conversion efficiency values, as the energy demand can be partially derived from thermal energy.

Considering the literature, this study couples a co-electrolyzer, FT synthesis, dual pressure swing adsorption, and a catalytic partial oxidation (CPOX) process for green syngas production. This efficient novel solution integrates various technologies as a suitable way to improve efficiency and couple thermal energy sources with the aim of reducing the electrical energy demand and promoting energy transition. For instance, CPOX is a catalytic process in which a feed containing a substoichiometric amount of oxygen is converted into syngas. This technology allows to produce green syngas using feedstock mixtures of flare gas, off-gas, tail gas, or biogas. Indeed, it can process a variety of resources such as renewables, Biogas or Biofuels, and refinery waste streams after the required desulfurization and purification treatments. In addition, CPOX reduces the temperature versus partial oxidation and relaxes the metallurgical requirements. Cleaner streams with feed sulfur contents below 50 ppm are required. The combination of syngas production technologies (co-electrolysis and CPOX) enables the maintenance of a constant optimum operating load in the FT synthesis reactor. Subsequently, syngas production can be modulated by regulating the degree of charge in the co-electrolyzer and CPOX reactor. As the output of the co-electrolysis process in the cathode outlet stream, unconverted CO_2 is still present; thus, high non-desired molar ratios could appear in the outlet stream. CO_2 does not react in the synthesis reactor; therefore, it must be removed. For this purpose, an integrated purification system for the syngas outlet of the co-electrolyzer was also included.

The remainder of this paper is organized as follows. Section Modeling methodology describes the proposed solution and the detailed system modeling. The modeling methodology is then presented with an overview of all the stages, including an additional description of each block and the corresponding selected operating parameters. The model results of the process for the selected case study are discussed in Section Result and discussion , which shows the breakdown of the process and equipment energy requirements, efficiency, and performance. A CPOX Reactor was integrated with SOEC stacks for heat recovery and steam generation in the waste-heat section (WHS). Thermal energy from the catalytic partial oxidation reactor outlet and the syngas stream was used to heat the inlets to the cathode and anode of the SOEC in the integration case. Finally, conclusions are presented in Section Conclusions.

Modeling methodology

Preliminaries: power-to-liquid process description

The (PtL) process uses renewable electricity as the key energy resource and captures CO_2 as feedstock [22,23], which can be generated through different pathways to produce liquid fuels in an FT synthesis reactor [24]. In the diagram shown in Fig. 1, two possible pathways and alternatives for the PtL process are presented. (i) Renewable H_2 is produced by electrolysis and CO_2 is incorporated into the stream and sent to the rWGS reactor for syngas production. (ii) Syngas is directly produced by co-electrolysis in a SOEC. Syngas was then conditioned and sent to the FT reactor for synthesis. Syncrude is upgraded to produce synthetic e-fuels, such as Kerosene, Gasoline or Diesel. The PtL process co-electrolysis integration path was analyzed as follows [25]: (i) co-electrolysis of H_2 and CO_2 to obtain syngas [26,27], a mixture of carbon monoxide (CO) and hydrogen (H_2); (ii) FT synthesis, conversion of synthesis gas into syngas; and (iii) upgrading, hydro-processing steps, hydrocracking, hydro-isomerization, and/or hydrogenation.

This study aimed to investigate the optimal integration of different novel technologies for green syngas generation and synthetic fuel production to mitigate the seasonality of renewables, maintain the independence of the electrical grid, and maximize the performance of the overall plant. For the proper modulation of syngas generation, CPOX has been studied for parallel coupling with co-electrolysis. This technology allows to produce green syngas using feedstock mixtures of flare gas, off-gas, tail gas, or biogas. Therefore, as shown in Fig. 1, the proposed solution is based on a co-electrolysis pathway.

General description

Electrolyzers demand large amounts of electric power for H_2 or syngas production; however, this energy is not always available because of seasonality and variations in daily production capacity. In contrast, the synthesis process and, in particular, the slurry bubble bed reactor require, for optimal operation, maintenance of the syngas feed flow inside the correct threshold, without major variations. Therefore, a constant supply of syngas is required under the conditions required by the reactor. In this study, the co-electrolyzer was coupled with a CPOX reactor, modulating syngas generation and performing thermal integration in such a way that the co-electrolyzer reached the thermoneutral operation mode with a reduction in power consumption. This technology allows to produce green syngas using feedstock mixtures of flare gas, off-gas, tail gas, or biogas. CPOX technology also allows the reduction of temperature versus partial oxidation and relaxes the required metallurgy.

A flowsheet model was developed using the sequential simulation software Aspen HYSYS®. Thermal analyses of the

Please cite this article as: Sánchez-Luján J et al., Optimal integration modeling of Co – Electrolysis in a power-to-liquid industrial process, International Journal of Hydrogen Energy, https://doi.org/10.1016/j.ijhydene.2023.07.012

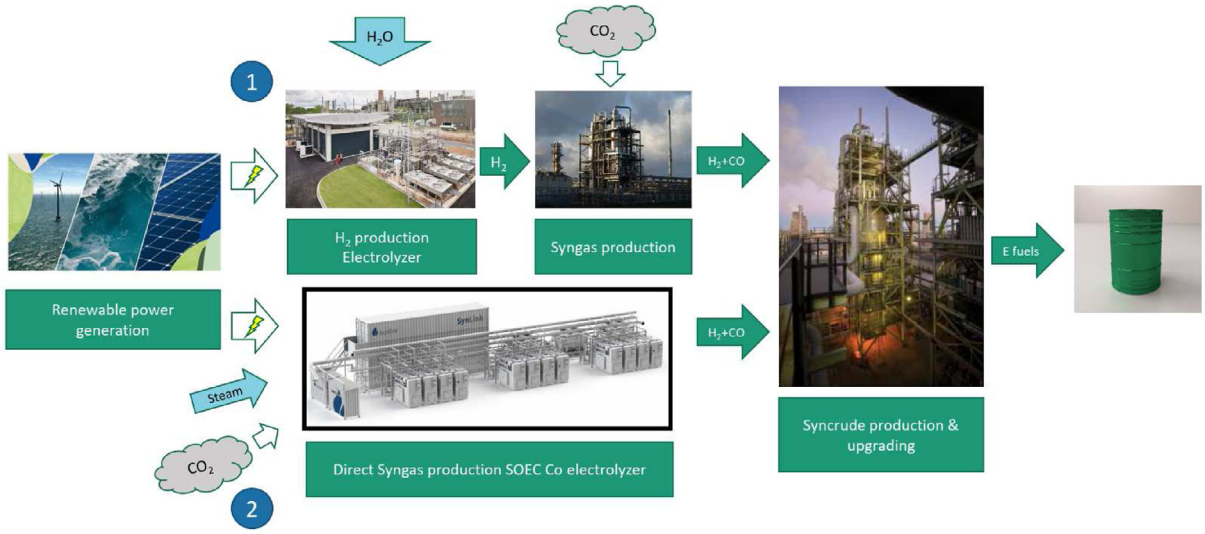

Fig. 1 – Power-to-liquid pathway block diagram of rWGS/co-electrolysis.

equipment and waste-heat recovery were performed to optimize the heat-integration network and estimate the required utilities at the battery limit. The model provides the interrelations among the units and their effects on the overall process. In addition, thermodynamic analysis was conducted based on the co-electrolysis of steam and CO_2 in a solid-oxide electrolyzer cell with FT synthesis. The flowsheet depicts the different process blocks; inputs, such as captured CO_2, Tail gas/flare gas/biogas, process water, and steam; and outputs, such as syngas and exported steam. The process is divided into several blocks: (i) the SOEC Inlet, where the feed points for steam, water, H_2 and CO_2 are also indicated at the cathode inlet, air electrode, and anode; (ii) syngas generation by the SOEC; (iii) synthesis, where syncrude is produced; (iv) pressure swing adsorption (PSA) islands for syngas purification and H_2 production; and (v) syngas cooling and CPOX, where heat integration is conducted.

In addition, different heat exchangers and waste-heat boilers (WHBs) for steam generation were included in the proposed solution. This heat-integrated system provides the feed steam required for the heating and cooling processes. With the steam generated in the internal coil of the Fischer–Tropsch reactor (FTR), the inlet syngas is heated to a reaction temperature of 240 °C [16]. The steam produced in the syngas cooling section was used for preheating the cathode and anode inlets [28,29]. To achieve the thermoneutral functioning mode [30], the final heating of the inlet cathode and anode up to 800 °C is performed with the syngas outlet stream produced in the CPOX reactor. The overall process is a steam exporter; furthermore, syngas produced in the CPOX reactor, with a H_2/CO ratio of 1.5, can also be exported to the industrial complex for other petrochemical processes or diverted into the synthesis unit.

Under the required conditions, the required utilities and feeds for plant operation are available at the battery limit. The main requirements and characteristics are as follows.

1 **Feedstock**. CO_2 was supplied from the capture plant under the required conditions, and desulfurization and purification were performed using less than 1 ppm of H_2S.
2 **Steam Generation**. Within the system, different heat exchangers and WHB were included for steam generation. This heat-integrated system is used to produce the feed steam required for the heating and cooling processes. The plant is considered a global steam export facility.
3 **Power Supply**. Medium-voltage (MV) AC power was supplied from the dedicated substation of the electrolyzer to the rectifier, and then converted into low-voltage (LV) CC for the Electrolyzer Stack. MV AC power for the compressors, chillers, and air coolers were supplied by an Industrial Complex Substation.
4 **Purified feedwater**. Water is used for steam production in the heat-integrated network and for hydrogen production in the SOEC. Water quality requirements are very specific, and any deviation can result in severe degradation of electrolyzer stacks.
5 **H_2** was continuously supplied by a recycling loop inside the SOEC to avoid oxidation of the Ni-based cathode.
6 **Auxiliaries**. Cooling water, and Boiled Feed Water are continuously required at the battery limit, as well as N_2 and steam, during startup and shutdown.

SOEC HT co–electrolysis operation

The SOEC model approach follows that outlined by Stoots et al. [29]. The yields were based on experimental analysis and data on the cathode effluent composition as a function of the stack operating current densities obtained in Ref. [30]. H_2O and CO_2 reduction occur at the fuel electrode and require an energy supply because of the endothermic properties of the reactions. Additionally, both reactions are related via endothermic reverse water–gas shift (rWGS) and CO methanation reactions, according to the following equations:

Please cite this article as: Sánchez-Luján J et al., Optimal integration modeling of Co – Electrolysis in a power-to-liquid industrial process, International Journal of Hydrogen Energy, https://doi.org/10.1016/j.ijhydene.2023.07.012

$H_2O \leftrightarrow H_2 + ½O_2$ ΔHr (860 °C) (+249 kJ/mol, H_2O reduction) (1)

$CO_2 \leftrightarrow CO + ½O_2$ ΔHr (860 °C) (+283 kJ/mol, CO_2 reduction) (2)

$H_2+CO_2 \leftrightarrow H_2O + CO$ ΔHr (860 °C) (+34 kJ/mol, rWGS) (3)

$CO + 3H_2 \leftrightarrow CH_4 + H_2O$ ΔHr (860 °C) (− 206.3 kJ/mol, CO methanation) (4)

The total energy demand (ΔH), as shown in Fig. 2, gradually increased for H_2O reduction and remained nearly constant for CO_2 reduction. For both the reactions, the electrical energy demand (ΔG) decreased with increasing temperature. The thermal energy demand (T·ΔS) increases with increasing temperature [31,32]. CO_2 reduction generally requires a higher amount of thermal (and total) energy supply, whereas the electrical energy demand is almost equal to water reduction at temperatures >750 °C. The additional thermal energy demand of the rWGS leads to lower stack temperatures and increased overpotential. SOECs operated in the pure CO_2 electrolysis mode have a higher thermoneutral voltage than those operated in the steam electrolysis mode because of the higher enthalpy of the reduction reaction. The high temperature electrolysis mode requires enthalpy of formation for the reactions to provide electrical and thermal energy.

The outlet gas composition shown in Fig. 3 was predicted accurately using the model outlined by Stoots et al. [29] and the experimental data reported by Aicart et al. [32]. The measured concentrations of the outlet gases are in accordance with the calculated thermodynamic equilibrium over the full range of current density. The experimental results of the gas analysis obtained by Riedel et al. [30] indicate that the rWGS and methanation reactions are fast and shift the gas mixture into equilibrium within the stack, see Fig. 3, even at high flow rates and a Reactant Conversion (RC) of 70%. High pressures, high H_2/CO ratios, and low temperatures are favorable for the CO methanation reaction. During the experiments performed by Riedel et al. [30], a methane content of almost 5% was measured at 8 bar and 790 °C for an inlet composition of 60/30/10 ($H_2O/CO_2/H_2$) with a H_2/CO ratio of 2.5 after 70% conversion.

At higher current densities, the methane content decreased owing to the increased stack temperature; thus, the H_2/CO ratio decreased. Within the conducted experiments, the H_2/CO ratio at the stack outlet is in a range of 1.18–1.27 for the inlet composition of 45/45/10 and between 2.31 and 2.48 for the 60/30/10 composition. As can be seen in Fig. 4, the core temperatures of the stack, experimental data sourced from Riedel et al. [30], decrease at low current densities because of the endothermic reduction reaction of H_2O, CO_2 and the endothermic rWGS reaction −data collected at 1.4 bar at a furnace temperature of 800 °C, RC = 70% inlet gas composition 60/30/10 ($H_2O/CO_2/H_2$). At higher current densities, the stack temperature increased owing to higher heat generation (or higher losses) [33,34].

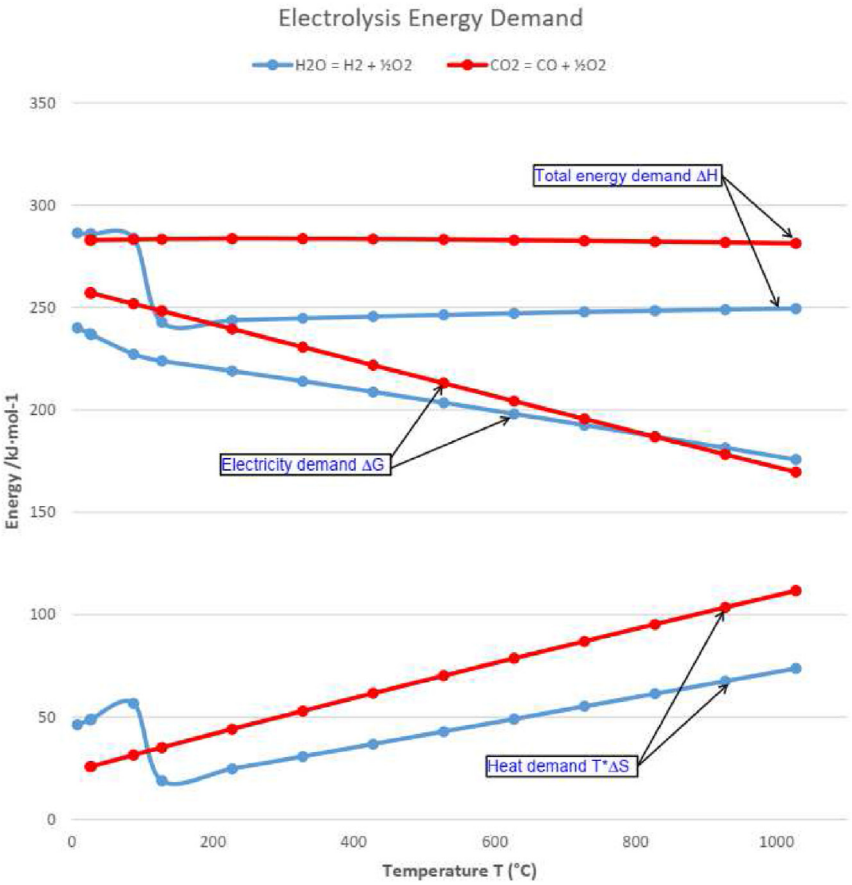

Fig. 2 – Energy demand for electrolysis.

Please cite this article as: Sánchez-Luján J et al., Optimal integration modeling of Co – Electrolysis in a power-to-liquid industrial process, International Journal of Hydrogen Energy, https://doi.org/10.1016/j.ijhydene.2023.07.012

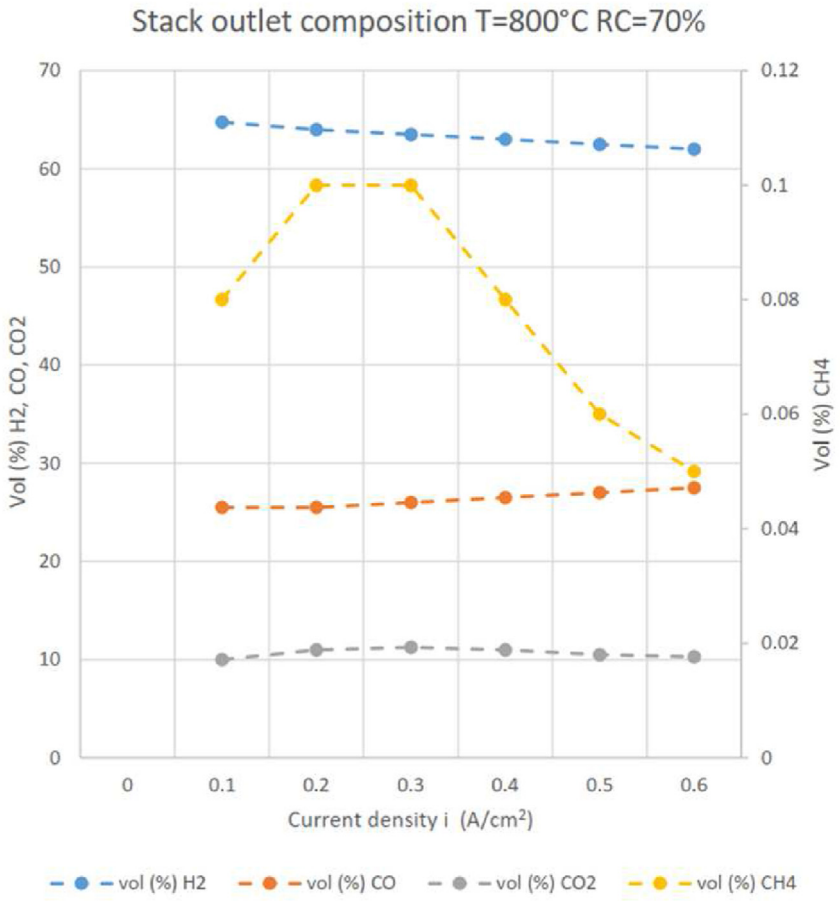

Fig. 3 – Gas analysis of stack outlet composition (experimental data).

The SOEC stack operates in a temperature range from 650 °C up to 1100 °C, the thermoneutral operating temperature is around 850 °C. Temperature fluctuation induces thermo-mechanical strains within the stack, leading to amplified fluctuations in current density, increasing the degradation rate, leaks likelihood, and ultimately resulting in malfunction of the stack [35–37]. Significant temperature fluctuations throughout the stack can lead to uneven cell deterioration, ultimately diminishing the stack's operational lifespan [38–40]. Consequently, it is ideal for the temperature variation within the stack to remain below 10 °C, literature proposes upper limits of 5–8 °C/cm for the temperature gradient across individual cells [27,41]. Shall be emphasized the importance of controlling and minimizing temperature variation in SOECs to improve durability and maximize stack lifespan. Further research and technological advancements are needed to address this challenge and enable large-scale implementation of SOEC technology, present SOEC stack designs exhibit temperature variations ranging from 50 to 80 °C, predominantly accepted by manufacturers [42,43].

SOEC heat integration

The syngas outlet stream of the CPOX reactor is integrated into the inlet streams of the cathode and anode of the SOEC to provide the required heat input; thus, to achieve in both inlet streams 800 °C, the thermal energy necessary to reach the thermoneutral operating mode. Fig. 5 illustrates the composite curves generated following the pinch point analysis methodology. It depicts the adopted strategies for recovering waste heat and the thermal integration with the Syngas stream generated in the CPOX reactor. Results are divided into three graphs due to the discontinuity of stream compositions as a consequence of several intermediate injections. In this way, the heat-integration details of the syngas outlet stream of the CPOX reactor, with inlet streams to the cathode and anode, are shown in Fig. 6. The process conditions for the SOEC inlet streams and the waste-heat recovery in the SOEC outlet streams are explained in detail below.

SOEC inlet

- Feed Mixing & Preheating, The required feed is mixed in the inlet of the SOEC to obtain the required syngas in the cathode outlet stream with the desired H_2/CO ratio of 2.1 for optimal conversion in a cobalt-based catalytic F–T reactor [16]. The feed was heated to achieve thermoneutral operation of the SOEC. Water and steam are mixed and preheated up to 550 °C in the heat exchangers, with the steam produced in the waste-heat section located in the syngas outlet line from the SOEC, see Fig. 6. The CO_2 was also preheated up to 375 °C, then the carbon dioxide/steam/hydrogen mix for feeding the Cathode SOEC was finally heated up to 800 °C with the outlet gas stream

Please cite this article as: Sánchez-Luján J et al., Optimal integration modeling of Co – Electrolysis in a power-to-liquid industrial process, International Journal of Hydrogen Energy, https://doi.org/10.1016/j.ijhydene.2023.07.012

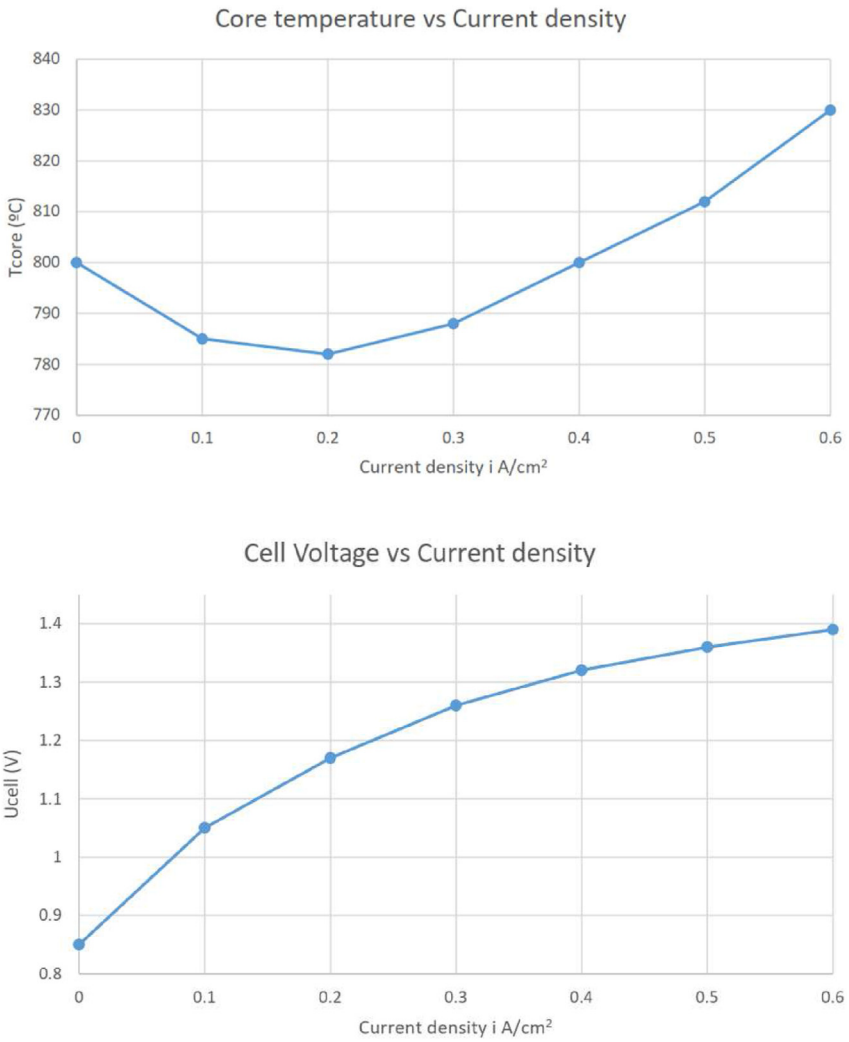

Fig. 4 – Steady-state core temperature and cell voltage versus current density (model prediction).

coming from the outlet of CPOX, catalytic partial oxidation Reactor, process condition pressure, and temperature are detailed in Table 1.

- Compressed Air to Anode, Air is compressed and pre-heated in a heat exchanger up to 224 °C and then heated downstream in two heat exchangers up to 800 °C before entering the air electrode with the Outlet Gas Stream coming from the CPOX reactor.

SOEC outlet

- Cathode, Fuel Electrode, The SOEC converts CO_2 and steam into a syngas-rich stream, and the syngas is cooled by the waste-heat recovery system and conditioned according to the PSA unit inlet requirements for purification of the syngas stream [14]. The PSA unit is represented in the flowsheet by a splitter that withdraws CO_2 and from the syngas stream, the CO_2 separated is recycled to the inlet again.
- Anode, Air Electrode, The sweep air stream is enriched with O_2, which is the product of the reduction reactions at the cathode and reaches the anode through the electrolyte. The outlet stream contained 50% oxygen and molar fraction. Air was used because of the high reactivity of pure oxygen, which prevents Cr deposition in the anode, thus degrading the SOEC.

Syngas conditioning

After purification, the syngas was compressed in several stages to achieve the required operating pressure for the FT synthesis reactor, with four compression stages of up to 4000 kPa. In accordance with API 618, the maximum discharge temperature for syngas is 300 °F/149 °C. The cooling system for the compressed syngas is shown in Fig. 6. At the inlet of the last compression stage, the recycled stream is mixed with the stream generated by co-electrolysis. This recycling originates from the PSA downstream of the F–T reactor, and this effluent is a consequence of the unreacted syngas fed to the reactor [44]. For the optimal operation of the cobalt-based catalyst F–T Reactor, the syngas is heated to a 240 °C inlet temperature by a heat exchanger, using the steam generated in the internal coil of the F–T Reactor [45].

Please cite this article as: Sánchez-Luján J et al., Optimal integration modeling of Co – Electrolysis in a power-to-liquid industrial process, International Journal of Hydrogen Energy, https://doi.org/10.1016/j.ijhydene.2023.07.012

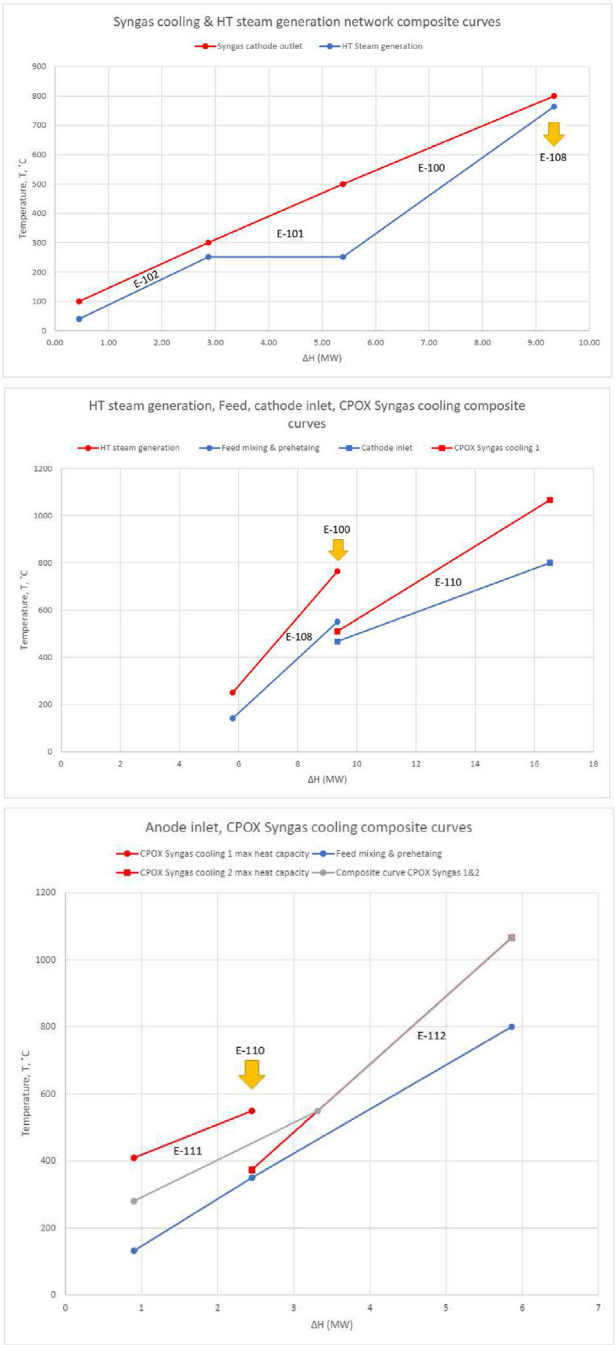

Fig. 5 – Composite curves of waste heat recovery and heat integration.

Fuel synthesis: fischer tropsch reactor

FT synthesis is a surface polymerization reaction of CO and H_2 that produces long-chain hydrocarbons, H_2O, and CO_2. The syncrude product contains n-paraffins and 1-olefins, but the distribution of the products depends on the process conditions, type of catalyst, and physical characteristics of the catalyst. There are two main types of FT syntheses, HTFT High temperature (300–350 °C) FT synthesis over catalysts active for the WGS reaction, such as iron-based catalysts and LTFT Low-temperature (200 – 240 °C) FT synthesis over non-shifting catalysts, such as cobalt.

In the present work, LTFT over a cobalt catalyst was studied because of its high paraffin fraction, which is suitable for jet/diesel fuel. Cobalt catalysts have higher activity, allowing for higher conversion in reasonable reactor volumes at low temperatures, and the cobalt catalysts used in LTFT are more stable with respect to deactivation than the iron catalysts used in HTFT.

FT reaction mechanisms. Kinetics and product distribution

A kinetic model based on the FTS Langmuir–Hinshelwood–Hougen–Watson (LHHW) for the surface polymerization reaction, formulating the rate equation for CO consumption, was selected. The model for the product distribution follows the ideal Anderson-Schulz-Flory (ASF) distribution and introduces corrections. The corrected ASF product distribution refers to refined version of the original ASF model that incorporates improved parameters, obtained by experimental data and customized models for different types of reactors and catalyst whose better describe the product distribution for Fischer-Tropsch synthesis in the case study [46,47]. The methane formation was substantially higher than that in the ideal ASF distribution. The ideal distribution could not explain the higher selectivity for methane, which was lower than the expected selectivity for ethylene. Regarding ethylene, the lower selectivity was primarily due to the lower stability of the ethylene intermediary species because of the lower activation energy or higher enthalpy of formation of the ethylene species compared with higher olefins [48]. The final product distribution shown in Fig. 7 has been obtained following the experimentally validated kinetic models of Pandey U et al. [45] and Rytter & Holmen [46].

The cobalt catalyst exhibited very little water–gas shift activity, but different amounts of CO_2 were formed in the FTS. Empirical results obtained by van Steen E et al. [49] provide evidence that the CO_2 selectivity increased with increasing partial pressure of water and decreased with increasing H_2/CO ratio. The formation of CO_2, even though the cobalt catalyst is WGS-inactive, is associated with the Co(II)O formed by the oxidation of the Co catalyst, which acts as a site for the WGS reaction [49,50]. Aspen HYSYS® is widely used in chemical engineering to model industrial processes. However, it does not provide a prebuilt block for the FT reactor. With this aim, a conversion reactor was selected, and the reaction set with stoichiometric coefficients were subsequently calculated: 32 reactions for the alkane CH_4 through $C_{30}H_{62}$, $C_{32}H_{66}$ and $C_{36}H_{74}$ were implemented. The fractional conversion of each reaction was calculated using the corrected ASF. The operating parameters of the FT reactor are listed in Table 2. The formation of oxygenates and aromatics was assumed to be negligible and the presence of these molecules was small in the LTFT. The overall CO conversion increased with the recycling configuration. Internal recycling leads to mixing of the FT reactor with fresh feed from the SOEC. The split fraction of the internal recycling was calculated from the predefined fraction of reactants in the FT feed gas, and the H2/CO ratio was determined by adjusting the amount of fresh CO2 feed in the process.

Please cite this article as: Sánchez-Luján J et al., Optimal integration modeling of Co – Electrolysis in a power-to-liquid industrial process, International Journal of Hydrogen Energy, https://doi.org/10.1016/j.ijhydene.2023.07.012

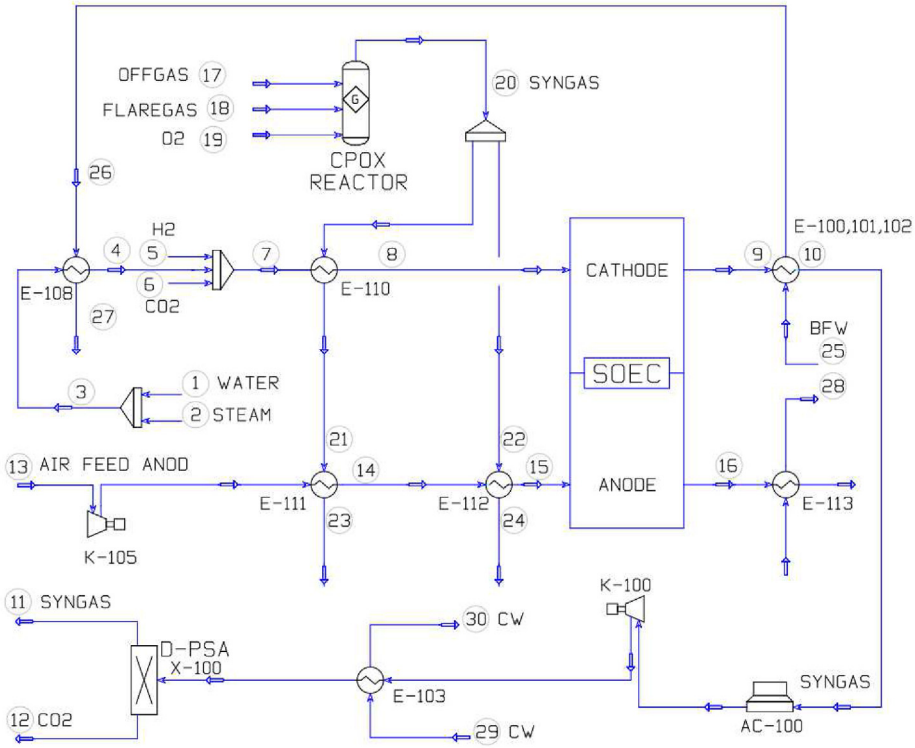

Fig. 6 – Flowsheet SOEC inlet heat-integration details.

Product separation and upgrading

The crude product was separated into four fractions. Therefore, these four steps were modeled and characterized by their boiling points and chemical compositions. The gaseous part of the syncrude, light fuel gas (LFG), and unreacted compounds were cooled stepwise and flashed, while the respective condensate was separated and forwarded as the product fraction. The temperature of the first flash vessel was set to 90 °C, and the condensate was sent to a 3-phase separator where longer hydrocarbons were separated from the water and aqueous condensate, as illustrated in the flowsheet of Fig. 8. Longer hydrocarbons include those with carbon numbers of up to C_{20}. In the second and third separation steps, the gases were cooled to 25 °C and 15 °C, respectively, and the lighter fractions were separated. The wax fraction was then sent to a hydrocracker for further upgrading. These waxes were compressed to the operation pressure of the hydrocracker, which was close to 6.0 MPa and preheated to the operation temperature of 350 °C. Hydrocracking is the catalytic cracking of long hydrocarbons into desired fuel fractions. The cracking reaction was conducted in the presence of H_2.

Table 1 – Flowsheet SOEC inlet heat-integration conditions.

No.	Stream	Temperature (°C)	Pressure (kPa)	No.	Stream	Temperature (°C)	Pressure (kPa)
1	Feed Water	30	180	**16**	O_2 Rich Air	800	170
2	Feed Steam	250	180	**17**	Off-gas Feed	40	1000
3	Steam Mix	141.8	180	**18**	Flare-gas Feed	40	1000
4	Steam	550	175	**19**	O_2 Feed	40	1000
5	Hydrogen	350	170	**20**	Syngas	1066	1000
6	CO_2	375	170	**21**	Syngas	549.2	995
7	Feed Mix	467.1	170	**22**	Syngas	1066	1000
8	Feed Mix	800	160	**23**	Syngas	409.1	990
9	Syngas	800	150	**24**	Syngas	373.7	995
10	Syngas	100	125	**25**	Boiler Feed Water (BFW)	40	4000
11	Syngas	80	990	**26**	Steam	763.8	3980
12	CO_2	80	220	**27**	Steam	250.9	3975
13	Air Feed Anod	30	100	**28**	Steam	403.9	3970
14	Air Feed Anod	350	195	**29**	Cooling Water (CW)	25	2000
15	Air Feed Anod	800	185	**30**	Cooling Water (CW)	80	1995

Please cite this article as: Sánchez-Luján J et al., Optimal integration modeling of Co – Electrolysis in a power-to-liquid industrial process, International Journal of Hydrogen Energy, https://doi.org/10.1016/j.ijhydene.2023.07.012

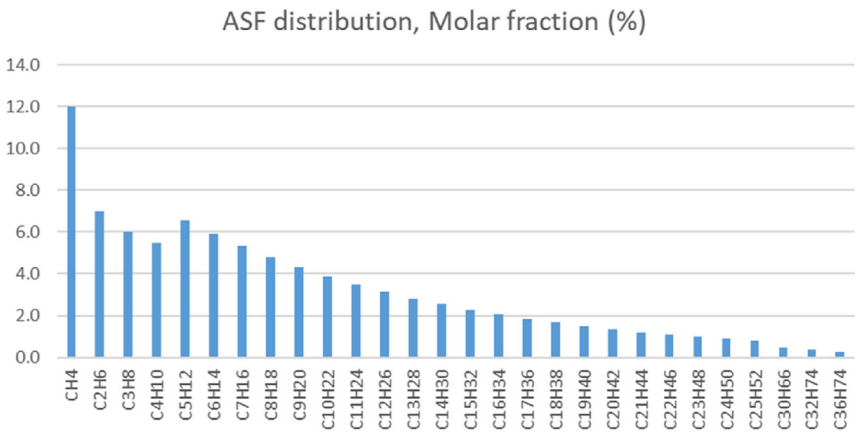

Fig. 7 – Corrected ASF distribution.

Table 2 – Main characteristics of the FTS reactor.

FT- Synthesis Reactor	
Parameter	Values
Chain growth probability	Olefins $\alpha = 0.9/\beta = 0.8$ Parafins
Methane correction Yield	0.12
Reaction Temperature	240 °C
Reaction Pressure	4000 kPa
H_2/CO Ratio	2.1
Total Conversion (over CO)	>75%
Reactor type	FT-Slurry Bubble Column Reactor
Catalyst	Cobalt based

Moreover, non-condensable LFG, with CH_4 and CO_2 converted in the FT reactor, was sent for dual PSA for syngas purification.

Dual pressure swing adsorption and recycling

Pressure Swing Adsorption (PSA) units are industry standards used worldwide for purifying synthesis gas in hydrogen plants and extracting hydrogen from valuable off-gases in refining process units. Hydrogen purity is typically greater than 99.9%, and low concentrations of carbon oxides (CO and CO_2) are required for downstream processing units. The feed gas enters the PSA unit at a high pressure; the product is delivered with a minimal pressure drop through the unit, whereas the tail gas is typically rejected at a low pressure. A PSA unit can be designed to accommodate a wide range of operating pressures, from low pressures (<100 psig) to units approaching 1000 psig. Tail gas pressures are typically 5 psig to maximize hydrogen recovery and can also be 75 psig or greater to match the plant's fuel header [51]. For the proposed solution, two different package units were considered: (i) a dual PSA for syngas purification, and (ii) a PSA for hydrogen production. The dual PSA sends purified syngas through the recycling loop to the inlet of the last stage of compression for FT reactor feeding, thus increasing the overall conversion of the unit. H_2 PSA supplied the required amount of hydrogen to the hydrocrackers [52].

The dual PSA process focuses on recovering syngas with a purity and recovery higher than 99% from LFG consisting of a mixture of CO_2, CH_4, CO, H_2, and other non-condensable products. Clean syngas can be recycled using an FT reactor, thereby increasing the overall conversion. The off-gas, mainly CO_2 and CH_4, was then sent to the CPOX reactor. The dual PSA process can also be used to recover the syngas contained in the tail gas of a H_2 purification PSA from the SMR-off-gas.

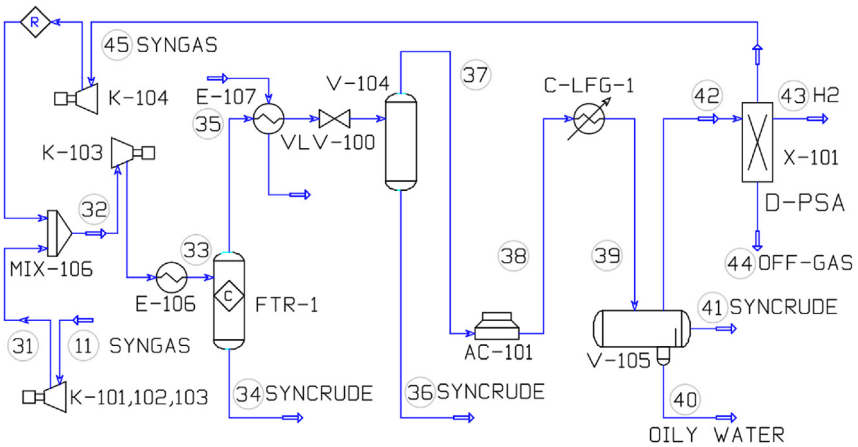

Fig. 8 – Flowsheet SOEC inlet heat-integration conditions.

Please cite this article as: Sánchez-Luján J et al., Optimal integration modeling of Co – Electrolysis in a power-to-liquid industrial process, International Journal of Hydrogen Energy, https://doi.org/10.1016/j.ijhydene.2023.07.012

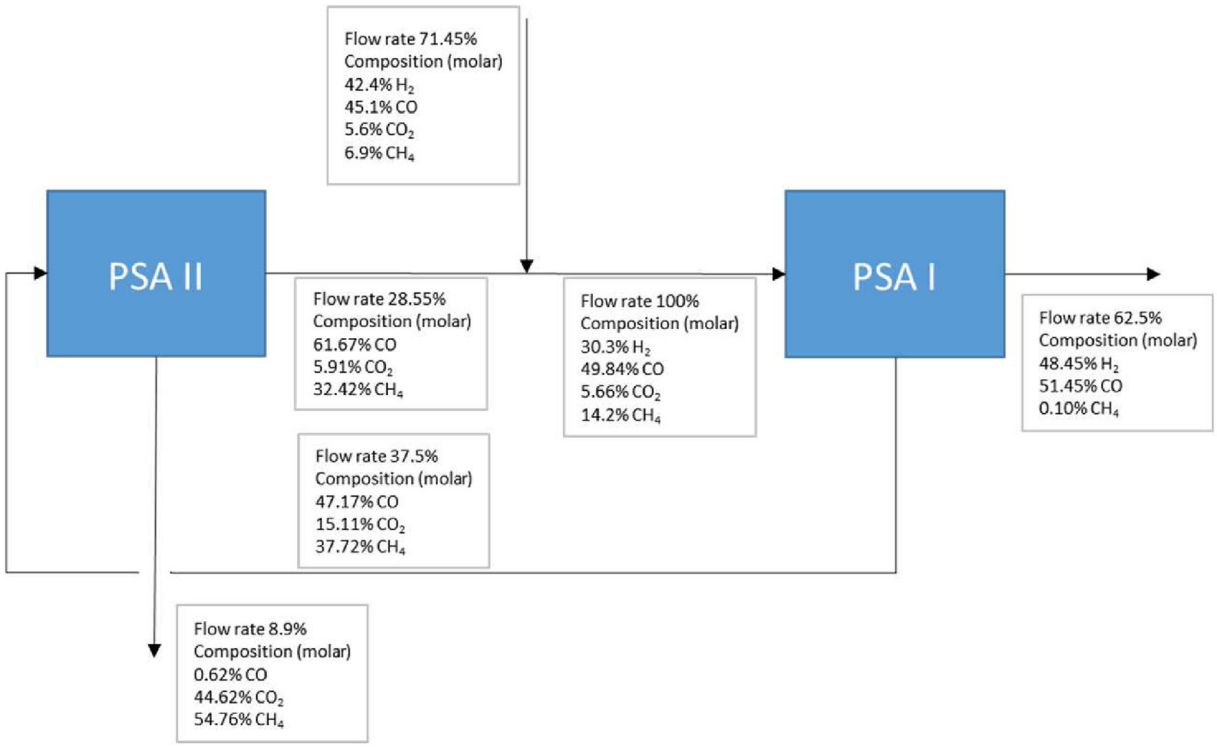

Fig. 9 – Flowsheet of the dual PSA.

Appropriate adsorbents for this application have a higher selectivity for CO_2 and lower selectivity for H_2 than the other gases involved, which is the key factor in the selection of the adsorbent for this application is CH_4/CO selectivity [53]. Activated carbon was selected as the adsorbent because of several reasons. The separation target is to obtain a syngas stream (formed by CO and H_2), withdrawing CO_2 and CH_4 in the Off-gas stream [54]. Dual PSA processes have a higher separation efficiency than single PSA processes. The dual PSA process included two coupled PSA cycles (PSA I and PSA II), as shown in Fig. 9. One cycle (PSA I) produced a raffinate enriched with light product. It also produces an extracted product (enriched in heavy products) that is fed into the second PSA cycle (PSA II). The light product of PSA II was mixed with fresh feed and the mixture was fed into PSA I. PSA I and PSA II cycles may involve different steps. Dual PSA was modeled as a splitter in the flowsheet, and the recovery and performance were based on the process outlined by Dobladez et al. [55].

Catalytic partial oxidation

CPOX is a catalytic process in which a feed containing a sub-stoichiometric amount of oxygen (or air) is catalytically converted into a CO + H_2 mixture. The use of a catalyst lowered the required reaction temperature to 800–900 °C. Commonly used catalysts include noble metal-based (Pt, Rh, Ir, and Pd) and non-noble–metal-based (Ni and Co) catalysts. Catalytic partial oxidation can be performed only if the sulfur content of the feed is below 50 ppm, as higher sulfur contents would poison the catalyst; in such cases, non-catalytic partial oxidation is more suitable use [56–58]. The CPOX reactor was integrated into the unit for several reasons.

- Syngas for fuel synthesis combined with SOECs is an attractive option for producing H_2 and CO. By simultaneously integrating both capacities, it is possible to modulate the production of syngas required for continuous

Table 3 – Flowsheet SOEC inlet heat-integration conditions.

No.	Stream	Temperature (°C)	Pressure (kPa)	No.	Stream	Temperature (°C)	Pressure (kPa)
11	Syngas	80	990	**38**	LFG	30	3150
31	Syngas	80	3000	**39**	LFG	15	2750
32	Syngas	73.1	3000	**40**	Oily Water	15	2750
33	Syngas	240	4000	**41**	Syncrude	15	2750
34	Syncrude	240	3400	**42**	LFG	15	2600
35	Syncrude	240	3400	**43**	Hydrogen	20	2550
36	Syncrude	90	3390	**44**	Off-Gas	20	1000
37	LFG	90	3390	**45**	Syngas	20	2550

Please cite this article as: Sánchez-Luján J et al., Optimal integration modeling of Co – Electrolysis in a power-to-liquid industrial process, International Journal of Hydrogen Energy, https://doi.org/10.1016/j.ijhydene.2023.07.012

Table 4 – Typical Flare gas composition.

Component	Volume fraction (%)	Weight fraction (%)
Methane- CH_4	81	60
Ethane – C_2H_6	5.5	7.7
Propane – C_3H_8	6.6	13.5
Butane – C_4H_{10}	4.0	10.8
Pentane – C_5H_{12}	1.4	4.8
Nitrogen - N_2	1.0	1.3
Carbon Dioxide – CO_2	0.17	0.33

Table 5 – CPOX reactor main operating conditions.

CPOX - Reactor	
Parameter	Values
Reaction Temperature	900 °C
Reaction Pressure	1000 kPa
Outlet Syngas H_2/CO Ratio	≈1.53
Reactor type	Catalytic
Catalyst	Nobel metal based/Ni Co based

plant operation by considering renewable power generation oscillations [56].

- In industrial complexes, feeds, such as flare gas, off-gas, and bioethanol, can be used. In rural or remote areas, other available feeds, such as biogas and pyrolysis oils, can be processed after the corresponding desulfurization and polishing processes, implementing circular economic principles [59–61]. Typical flare gas compositions are listed in Table 3.
- The outlet stream of the high temperature syngas is produced in the reaction and through a heat exchanger, allowing heating of the SOEC electrolyzer feed, both the anode and cathode. The CPOX syngas outlet stream is sent to a dual PSA for syngas purification.

A Gibbs reactor is used in the proposed solution. The Gibbs reactor of Aspen HYSYS® can function solely as a separator. In a reactor that minimizes the Gibbs free energy without an attached reaction set or as a reactor using equilibrium reactions, the output is very similar to that of an equilibrium reactor [62,63]. The operating conditions of the reactor and the inlet composition of the flare gas is listed in Tables 4 and 5, respectively. A sensitivity study was conducted to minimize O_2 consumption and maximize methane conversion, that is hydrogen production.

Results and discussion

Case study

Owing to the synergies related to the integration of high temperature heat with the CPOX process for green syngas generation, the proposed solution was based on a co-electrolysis pathway for syngas production. In this case study, the plant production capacity was determined by a power availability of 100 MW from renewable power generation units, combining onshore and offshore wind power plants, and PV solar installations. Moreover, the capacity of the plant is fixed by the capacity of the electrolyzer (up to 100 MW DC), which is in line with the average capacity of the electrolyzers to be installed in the EU Hydrogen Valleys [64] and agrees with the capacity of the renewable power generation system. Syngas is produced by co-electrolysis provided by these renewables in the CPOX reactor. The mass flow of

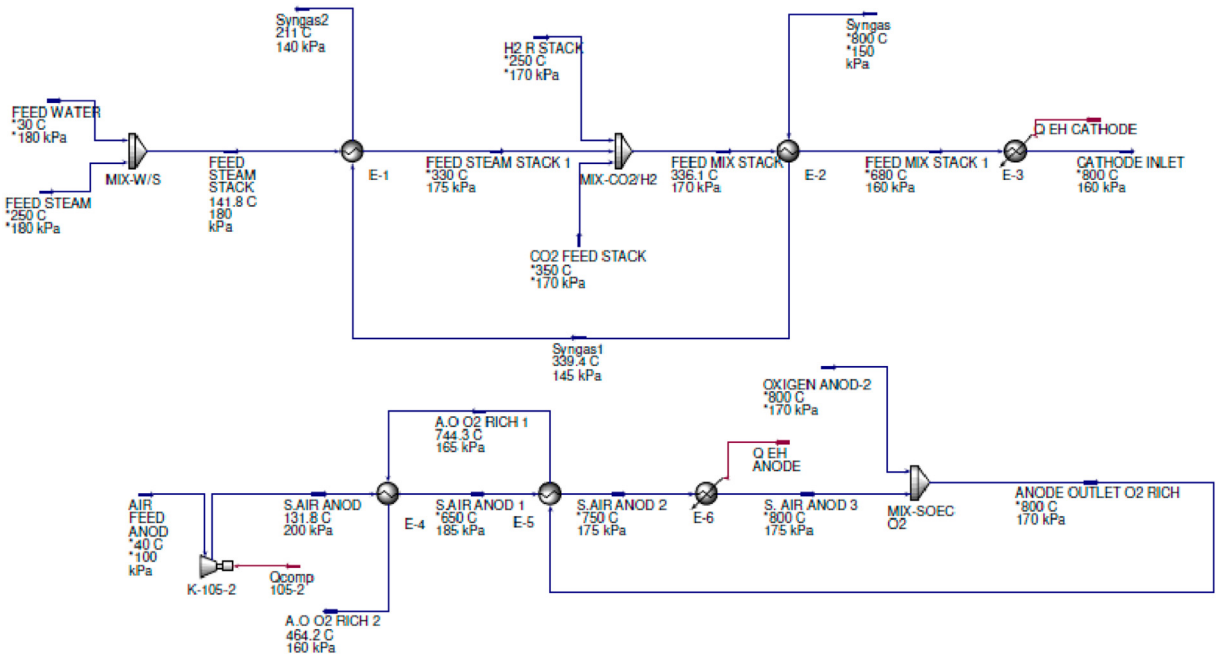

Fig. 10 – Base case for heat recovery in SOEC.

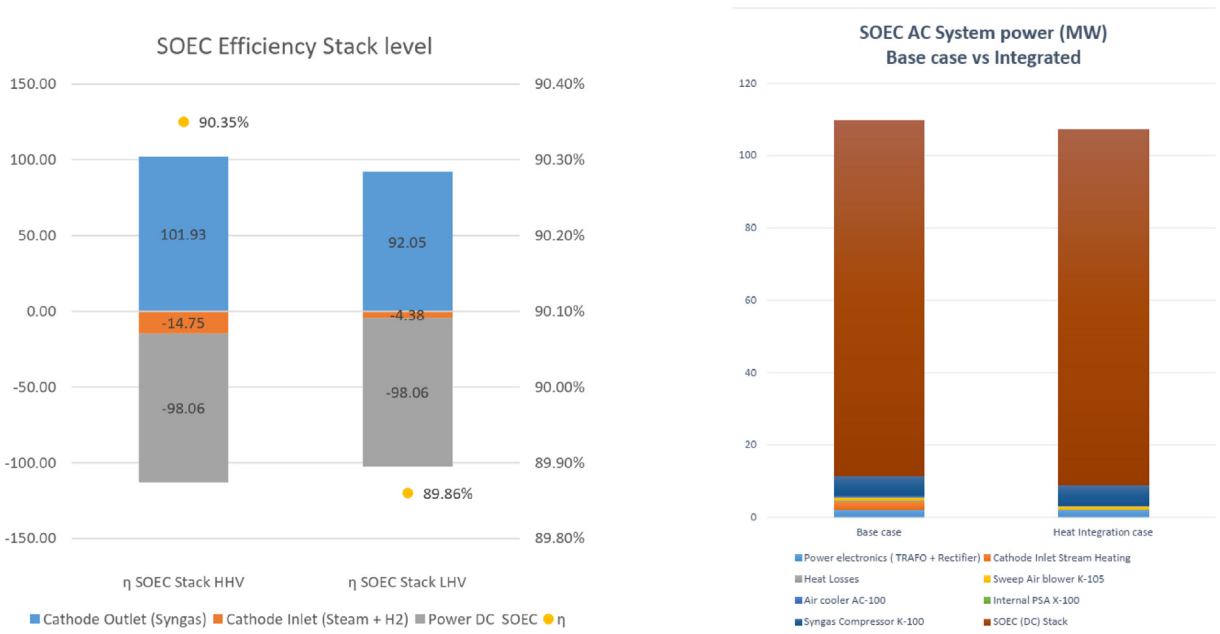

Fig. 11 – SOEC efficiency stack level and base case vs heat integrated power consumption.

syngas generated in the co-electrolyzer was calculated from the available renewable power generation (100 MW). The H_2 required for upgrading was generated by an independent SOEC and considered as an additional input. CO_2 at the battery limit was provided in. 2.5 MPa, which was consistent with the required inlet pressure. Then, the stream of syngas produced in the co-electrolyzer is cooled down up to optimal Fischer–Tropsch reaction temperature around 240 °C and fed to the FT reactor. Subsequently, gaseous and liquid output streams, LFG, and syncrude are generated.

The liquid product stream was sent to the hydrocracker and the gaseous stream was cooled simultaneously. The final gas stream was composed of hydrocarbons (HC), CO, H_2, and CO_2. The light waxes were combined with the liquid syncrude and supplied to the upgraded section. The hydrocracker product was flashed under ambient conditions. The liquid products from the separation sections were collected and brought to ambient conditions. These liquid streams were mixed to form the final liquid fuels, in line with the methodology proposed in Section Modeling methodology.

SOEC electrolyzer

The design of the unit to produce syngas by co-electrolysis focuses on obtaining a stream of syngas with an H_2/CO ratio of 2.1 with a minimum content of methane, and free of CO_2. Synthesis processes for obtaining other valuable products, such as methanol or synthetic methane, require syngas with different stoichiometric compositions for the methanation process $\frac{[H_2]-[CO_2]}{[CO]+[CO_2]} = 3$; for methanol $\frac{[H_2]-[CO_2]}{[CO]+[CO_2]} = 2.1$. Therefore, at

Table 6 – SOEC efficiency system level, base case, and heat integrated.

SOEC Efficiency System Level	BASE CASE		HEAT INTEGRATION	
	MW(HHV)	MW(LHV)	MW(HHV)	MW(LHV)
Cathode Outlet (Syngas)	**101.93**	**92.05**	**101.93**	**92.05**
Cathode Inlet (Steam + $H_{2\ \text{Cathode red}}$)	**14.75**	**4.38**	**14.75**	**4.38**
Steam	9.63	0.00	9.63	0.00
$H_{2\ \text{Cathode red}}$	5.13	4.38	5.13	4.38
Power AC SOEC System	**107.16**	**107.16**	**107.11**	**107.11**
P DC SOEC Stack	98.06	98.06	98.06	98.06
Power electronics (TRAFO + Rectifier)	2.19	2.19	2.14	2.14
Sweep Air blower K-105	0.88	0.88	0.88	0.88
Air cooler AC-100	0.45	0.45	0.45	0.45
Internal PSA X-100	0.02	0.02	0.02	0.02
Syngas Compressor K-100	5.56	5.56	5.56	5.56
Inlet Electrical Heating	**2.44**	**2.44**	**0.00**	**0.00**
Cathode Inlet Stream Heating	2.24	2.24	0.00	0.00
Heat Losses	0.20	0.20	0.00	0.00
η system level	**82%**	**81%**	**84%**	**83%**

Please cite this article as: Sánchez-Luján J et al., Optimal integration modeling of Co – Electrolysis in a power-to-liquid industrial process, International Journal of Hydrogen Energy, https://doi.org/10.1016/j.ijhydene.2023.07.012

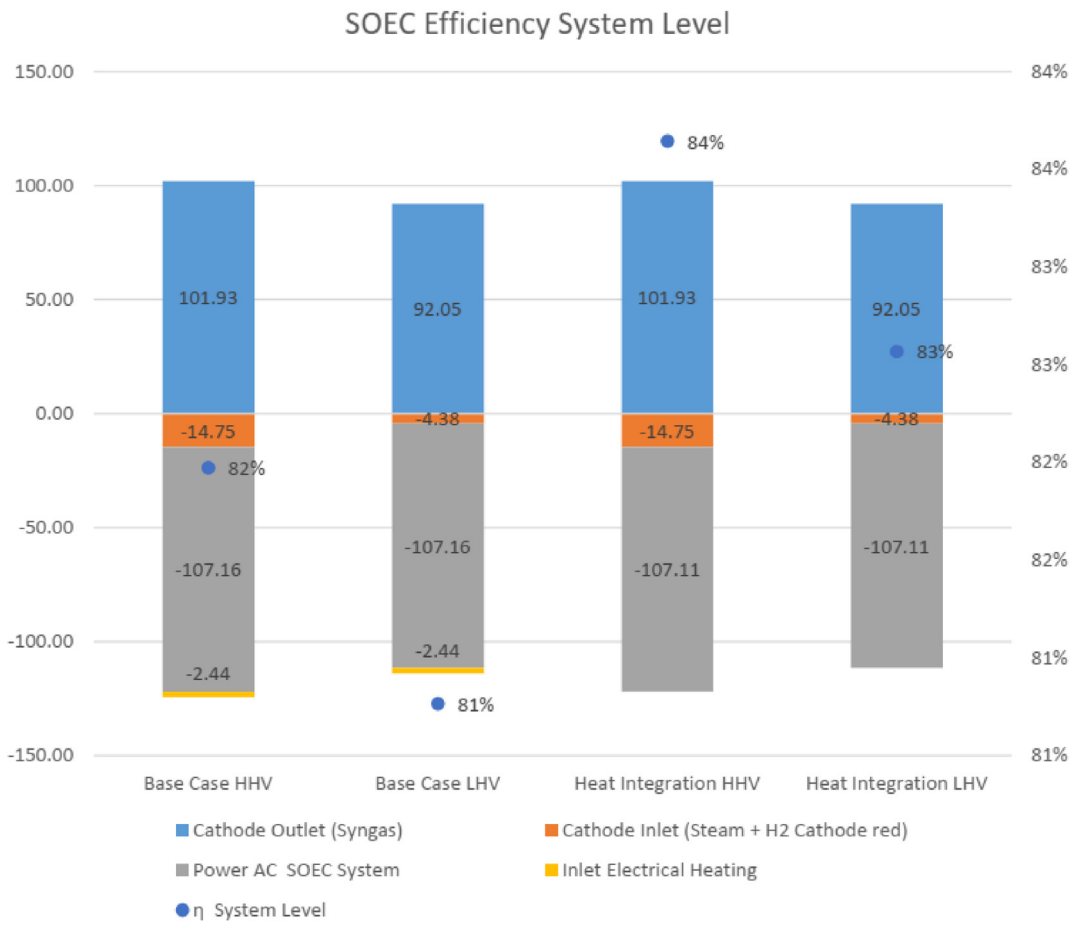

Fig. 12 – SOEC efficiency system-level base case vs heat-integrated cases.

the unit level, conditioning is considered necessary in terms of pressure and temperature for integration with the required PSA for syngas purification prior to the compression stages until the required pressure in the FT reactor is reached [65]. The heat necessary for conditioning all feeds (water, steam, CO_2, CO_2 recycled, and recycled H_2) is produced within the plant. For plants in industrial complexes, thermal integration is complex and nontrivial, requiring a balanced approach between the production of steam for export and the use of process currents between different blocks/units. Pinch-point analysis was performed for optimal use. A base case was developed to establish a baseline and to measure the benefits and improvements of the process and heat integration. The performance results of the base and present cases with heat integration are presented below, highlighting efficiency improvements. A flowsheet for the baseline cases of the cathode and anode of the SOEC is shown in Fig. 10. The results of the efficiency study at the stack and system levels of the SOEC are summarized in Fig. 11. Analyzing the base configuration for the actual capacity of the plant and achieving the required inlet temperature of 800 °C, it is necessary to supply an additional thermal power of 2.44 MW, as shown in Table 6.

In the case of integration in an industrial complex, all the thermal energy necessary to reach the thermoneutral operating mode of the stack was supplied through heat recovery and thermal integration of the process streams, thus allowing us to achieve a 2% higher performance at all levels for the studied capacity. The SOEC efficiency (HHV) at the system level was 84% (Fig. 12), supplying syngas and clean CO_2 at a

Table 7 – SOEC efficiency stack level.

SOEC Efficiency Stack Level	MW(HHV)	MW(LHV)
Cathode Outlet (Syngas)	101.93	92.05
Cathode Inlet (Steam + $H_{2\ Cathode\ red}$)	14.75	4.38
Steam	9.63	0
$H_{2\ Cathode\ red}$	5.13	4.38
Power DC SOEC	98.06	
η stack level	**90.35%**	**89.86%**

Table 8 – Fischer Tropsch efficiency system level and efficiency to Syncrude.

Fischer Tropsch Efficiency System Level	MW(HHV)	MW(LHV)
FT Reactor Outlet	93.26	82.22
FT Liquid Reactor Outlet	57.49	49.91
Syngas Inlet to FT Reactor	111.29	100.26
Syngas Compressors AC Power	3.95	3.95
Syncrude Cooling AC Power	1.16	1.16
LFG purification AC Power	0.04	0.04
η FT sytem level	**80.1%**	**78.0%**
η FTL system level, yield to Liquid	**49.4%**	**47.4%**

Please cite this article as: Sánchez-Luján J et al., Optimal integration modeling of Co – Electrolysis in a power-to-liquid industrial process, International Journal of Hydrogen Energy, https://doi.org/10.1016/j.ijhydene.2023.07.012

pressure of 990 kPa. The detailed energy consumption is listed in Tables 6 and 7.

FTS fischer tropsch synthesis and CPOX process

To calculate the efficiency of the conversion process for synthetic crude oil, all required compression stages were considered and included in the model to reach a reactor working pressure of 4000 kPa. Therefore, all the electrical consumption necessary for the stages of cooling and flashing of synthetic crude are considered for simulations, as well as purification and recycling. The detailed breakup and calculation results are presented in Table 8. The conversion of synthetic crude oil to liquid distillate fuels, jet fuel, diesel, and gasoline, which are obtained by passing through isomerization units, hydrocrackers, etc., was not covered in this study. The process achieved an HHV efficiency of 49% for the liquid (syncrude). The power required for the water effluent treatment generated in the synthesis process is not included in the efficiency calculation because the plant is integrated into an industrial complex. The treatment would be conducted with the rest of the complex effluents in a common waste treatment plant and will be considered utility consumption.

The CPOX reactor system generates approximately 20 Mton/h of syngas with $H_2/CO \approx 1.6$, and the outlet stream of the reactor (1000 °C) is heat integrated with the feed inlet streams of the cathode and anode of the SOEC co-electrolyzer, achieving the thermoneutral operation mode without additional heat supply. Subsequently, to calculate the efficiency of syngas production by the catalytic partial oxidation reactor, purification using dual PSA was performed. The feed streams, outputs, and efficiencies are presented in Table 9.

Table 9 – CPOX efficiency system level.

CPOX Efficiency System Level	MW(HHV)	MW(LHV)
CPOX System Outlet	**131.36**	**119.61**
Syngas	129.12	117.81
Offgas	2.24	1.79
CPOX Reactor Inlet	**149.03**	**136.29**
Desulphurized Flaregas	123.57	113.01
PSA + DPSA Offgas	25.46	23.29
Power Oxigen separation	1.8	1.8
Syngas purification DPSA	0.04	0.04
η CPOX sytem level	**87.1%**	**86.6%**

Table 10 – Overall Plant efficiency.

Plant Efficiency	MW(HHV)	MW(LHV)
Total Power AC in	**114.40**	**114.40**
Desulphurized Flaregas	**123.57**	**113.01**
H_2 Cathode Red	**5.26**	**5.26**
Plant outputs	**189.70**	**170.26**
CPOX Syngas	131.36	119.61
H_2 PSA	0.86	0.74
Liquid Syncrude	57.49	49.91
η Plant level	**78.0%**	**73.2%**

Plant efficiency, syngas production, and syncrude generation

The total plant efficiency was estimated to be 78% (73.2%LHV basis) for the combined syngas and syngas generation when 115 MW of AC electricity was supplied, as shown in Table 10. The steam cycle efficiency, which converts the electricity produced on a heat input basis, does not account for the overall efficiency, and the exported steam is separately considered as a plant output owing to the high interest in this

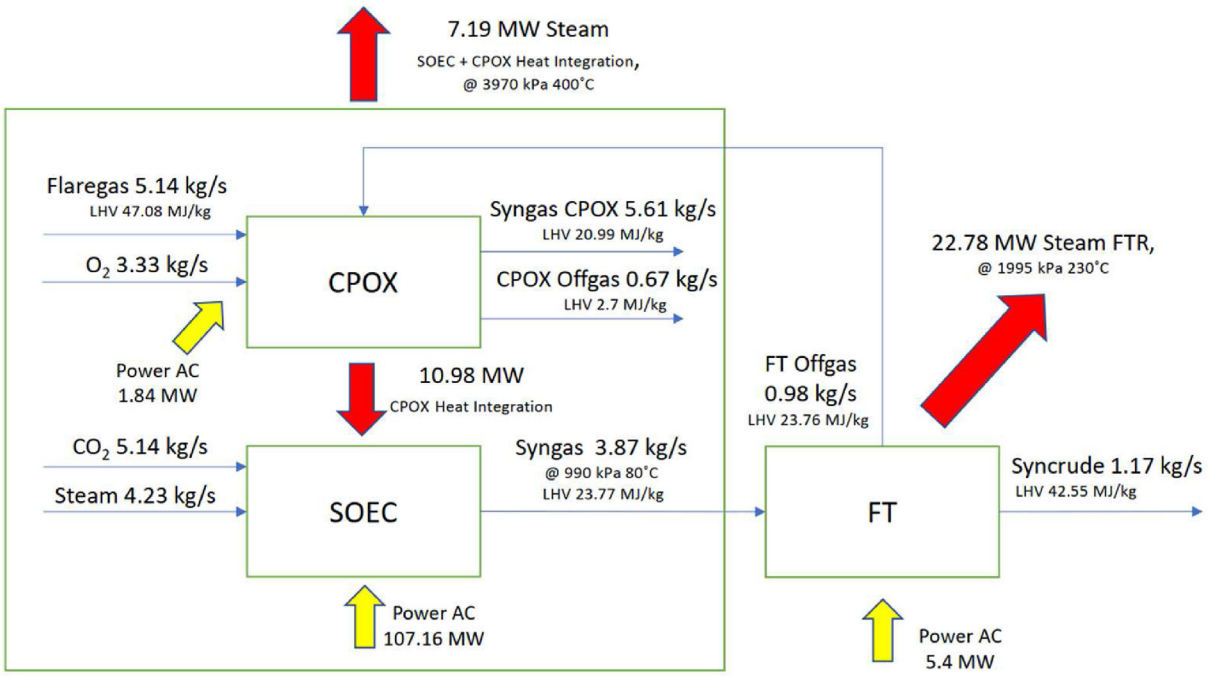

Fig. 13 – Mass and energy process using block diagram.

Please cite this article as: Sánchez-Luján J et al., Optimal integration modeling of Co – Electrolysis in a power-to-liquid industrial process, International Journal of Hydrogen Energy, https://doi.org/10.1016/j.ijhydene.2023.07.012

utility for integration in different processes in the industrial complex, where the steam is a valuable and highly demanded heat carrier for many processes. The total steam generation capacity was 30 MW, as explained in detail in Fig. 13. The total plant efficiency accounts for the energy inputs and outputs of the plant, except for the generated steam, heat output, net power required, and heating value of the liquid syncrude and generated syngas (HHV basis).

The indicated mass flow rate for the Syncrude in Fig. 13 is collected in several product fractions. The FT Off-gas is a Methane and CO_2 rich stream while CPOX Off-gas is very low heating value tail-gas obtained from purification of the Syngas produced in the Catalytic Partial Oxidation Reactor.

Conclusions

In this study, an integrated process for syncrude and syngas production on an industrial scale was described and assessed. The integrated process model includes a co-electrolyzer, Fischer–Tropsch reactor, dual PSA and CPOX Reactor, incorporating novel and efficient technologies, while utilizing residual streams as feed, renewable power, and captured CO_2. The configuration of the process is flexible and allows for adjustment of the amount of synthesis gas exported in such a way that the synthesis unit is kept operating at full capacity, depending on the needs of the industrial complex and the availability of renewable power. The stoichiometric ratios of H_2/CO and $(H_2 - CO_2)/(CO + CO_2)$ required for the subsequent synthesis processes can be adjusted by the production of hydrogen in the SOEC electrolyzer modules. Thus, the co-electrolyzers have a modular architecture and the regulation of the load depends on the production of renewables, which is achieved by coupling modules, regulating the load operating point, and maximizing performance. The output of the catalytic partial oxidation reactor was adjusted via load regulation. For the optimal operation of both technologies to produce green syngas and maximize the efficiency of the plant, thermal integration of the process streams was proposed and assessed.

A thermodynamic analysis of the benchmark versus the integration scheme in the SOEC co-electrolyzer with the CPOX reactor revealed that electrical efficiencies of 82% and 84% could be achieved at the system level, thus increasing the efficiency by 2%. The impacts of some key parameters, such as current density and operating temperature on the system performance, were also investigated. The system realized optimized parameters of current density and operating temperature, which let to improved performance. Remarkably, a power-to-liquid efficiency of 49 was achieved for syncrude, and the overall plant efficiency was 78%. The synthesis unit can export approximately 30 MW of MP steam.

In future studies, the integration of mixed ionic–electronic conducting membranes (MIEC) for oxygen separation from the outlet stream of sweep air (O_2 rich) from the anode of the SOEC electrolyzer will allow the unit to be independent of the oxygen supply and increase the overall performance. Additionally, the sweep air stream after oxygen depletion can be partially recirculated, thereby reducing the required thermal energy input. MIEC typically separates oxygen from air at high temperatures (800–900 °C). Moreover, the overall plant AI based optimization study is currently under development, from which the research results will published. Modes of operation and advanced control philosophy of the plant are included in the scope of the study.

Declaration of competing interest

The authors declare that they have no known competing financial interests or personal relationships that could have appeared to influence the work reported in this paper.

Acknowledgements

The authors acknowledge the project funded by the Comunidad Autónoma de la Región de Murcia, Consejería de Desarrollo Económico, Turismo y Empleo (Región de Murcia, Spain), and the European Union through the program RIS3-MUR (Ref:2I20SAE00079).

REFERENCES

[1] Boie I, Fernandes C, Frías P, Klobasa M. Efficient strategies for the integration of renewable energy into future energy infrastructures in Europe – an analysis based on transnational modeling and case studies for nine European regions. Energy Pol 2014;67:170–85. https://doi.org/10.1016/J.ENPOL.2013.11.014.

[2] Kovač A, Paranos M, Marciuš D. Hydrogen in energy transition: a review. Int J Hydrogen Energy 2021;46:10016–35. https://doi.org/10.1016/J.IJHYDENE.2020.11.256.

[3] Davis SJ, Lewis NS, Shaner M, Aggarwal S, Arent D, Azevedo IL, et al. Net-zero emissions energy systems. Science 2018;360. https://doi.org/10.1126/SCIENCE.AAS9793. 1979.

[4] Kaiser P, Unde RB, Kern C, Jess A. Production of liquid hydrocarbons with CO $_2$ as carbon source based on reverse water-gas shift and fischer-tropsch synthesis. Chem Ing Tech 2013;85:489–99. https://doi.org/10.1002/cite.201200179.

[5] Wang M, Wang G, Sun Z, Zhang Y, Xu D. Review of renewable energy-based hydrogen production processes for sustainable energy innovation. Global Energy Interconnection 2019;2:436–43. https://doi.org/10.1016/j.gloei.2019.11.019.

[6] Weitemeyer S, Kleinhans D, Vogt T, Agert C. Integration of Renewable Energy Sources in future power systems: the role of storage. Renew Energy 2015;75:14–20. https://doi.org/10.1016/j.renene.2014.09.028.

[7] Hänggi S, Elbert P, Bütler T, Cabalzar U, Teske S, Bach C, et al. A review of synthetic fuels for passenger vehicles. Energy Rep 2019;5:555–69. https://doi.org/10.1016/j.egyr.2019.04.007.

[8] Singh S, Jain S, Ps V, Tiwari AK, Nouni MR, Pandey JK, et al. Hydrogen: a sustainable fuel for future of the transport sector. Renew Sustain Energy Rev 2015;51:623–33. https://doi.org/10.1016/J.RSER.2015.06.040.

[9] Wilhelm DJ, Simbeck DR, Karp AD, Dickenson RL. Syngas production for gas-to-liquids applications: technologies, issues and outlook. Fuel Process Technol 2001;71:139–48. https://doi.org/10.1016/S0378-3820(01)00140-0.

[10] Wang L, Pérez-Fortes M, Madi H, Diethelm S, herle J van, Maréchal F. Optimal design of solid-oxide electrolyzer based

power-to-methane systems: a comprehensive comparison between steam electrolysis and co-electrolysis. Appl Energy 2018;211:1060–79. https://doi.org/10.1016/J.APENERGY.2017.11.050.

[11] Santos RG dos, Alencar AC. Biomass-derived syngas production via gasification process and its catalytic conversion into fuels by Fischer Tropsch synthesis: a review. Int J Hydrogen Energy 2020;45:18114–32. https://doi.org/10.1016/j.ijhydene.2019.07.133.

[12] Liu Z, Masel RI, Chen Q, Kutz R, Yang H, Lewinski K, et al. Electrochemical generation of syngas from water and carbon dioxide at industrially important rates. J CO2 Util 2016;15:50–6. https://doi.org/10.1016/j.jcou.2016.04.011.

[13] Yang Z, Wu Y, Zhang Z, Li H, Li X, Egorov RI, et al. Recent advances in co-thermochemical conversions of biomass with fossil fuels focusing on the synergistic effects. Renew Sustain Energy Rev 2019;103:384–98. https://doi.org/10.1016/J.RSER.2018.12.047.

[14] Delgado Dobladez JA, Águeda Maté VI, Torrellas SÁ, Larriba M, Brea P. Efficient recovery of syngas from dry methane reforming product by a dual pressure swing adsorption process. Int J Hydrogen Energy 2021;46:17522–33. https://doi.org/10.1016/J.IJHYDENE.2020.02.153.

[15] Gupta PK, Kumar V, Maity S. Renewable fuels from different carbonaceous feedstocks: a sustainable route through <scp>Fischer–Tropsch</scp> synthesis. J Chem Technol Biotechnol 2021;96:853–68. https://doi.org/10.1002/jctb.6644.

[16] Becker WL, Braun RJ, Penev M, Melaina M. Production of Fischer–Tropsch liquid fuels from high temperature solid oxide co-electrolysis units. Energy 2012;47:99–115. https://doi.org/10.1016/j.energy.2012.08.047.

[17] Herz G, Rix C, Jacobasch E, Müller N, Reichelt E, Jahn M, et al. Economic assessment of Power-to-Liquid processes – influence of electrolysis technology and operating conditions. Appl Energy 2021;292. https://doi.org/10.1016/j.apenergy.2021.116655.

[18] Tremel A, Wasserscheid P, Baldauf M, Hammer T. Techno-economic analysis for the synthesis of liquid and gaseous fuels based on hydrogen production via electrolysis. Int J Hydrogen Energy 2015;40:11457–64. https://doi.org/10.1016/j.ijhydene.2015.01.097. Elsevier Ltd.

[19] König DH, Baucks N, Dietrich RU, Wörner A. Simulation and evaluation of a process concept for the generation of synthetic fuel from CO2 and H2. Energy 2015;91:833–41. https://doi.org/10.1016/j.energy.2015.08.099.

[20] Wang L, Chen M, Küngas R, Lin TE, Diethelm S, Maréchal F, et al. Power-to-fuels via solid-oxide electrolyzer: operating window and techno-economics. Renew Sustain Energy Rev 2019;110:174–87. https://doi.org/10.1016/j.rser.2019.04.071.

[21] Wang F, Wang L, Ou Y, Lei X, Yuan J, Liu X, et al. Thermodynamic analysis of solid oxide electrolyzer integration with engine waste heat recovery for hydrogen production. Case Stud Therm Eng 2021;27. https://doi.org/10.1016/j.csite.2021.101240.

[22] Luo Y, Shi Y, Li W, Cai N. Comprehensive modeling of tubular solid oxide electrolysis cell for co-electrolysis of steam and carbon dioxide. Energy 2014;70:420–34. https://doi.org/10.1016/J.ENERGY.2014.04.019.

[23] Liu Z, Masel RI, Chen Q, Kutz R, Yang H, Lewinski K, et al. Electrochemical generation of syngas from water and carbon dioxide at industrially important rates. J CO2 Util 2016;15:50–6. https://doi.org/10.1016/j.jcou.2016.04.011.

[24] Wang L, Chen M, Küngas R, Lin TE, Diethelm S, Maréchal F, et al. Power-to-fuels via solid-oxide electrolyzer: operating window and techno-economics. Renew Sustain Energy Rev 2019;110:174–87. https://doi.org/10.1016/j.rser.2019.04.071.

[25] van Bavel S, Verma S, Negro E, Bracht M. Integrating CO_2 electrolysis into the gas-to-liquids–power-to-liquids process. ACS Energy Lett 2020;5:2597–601. https://doi.org/10.1021/acsenergylett.0c01418.

[26] Küngas R. Review—electrochemical CO 2 reduction for CO production: comparison of low- and high-temperature electrolysis technologies. J Electrochem Soc 2020;167:044508. https://doi.org/10.1149/1945-7111/AB7099.

[27] Hauch A, Traulsen ML, Küngas R, Skafte TL. CO2 electrolysis – gas impurities and electrode overpotential causing detrimental carbon deposition. J Power Sources 2021;506. https://doi.org/10.1016/j.jpowsour.2021.230108.

[28] Jensen SH, Sun X, Ebbesen SD, Knibbe R, Mogensen M. Hydrogen and synthetic fuel production using pressurized solid oxide electrolysis cells. Int J Hydrogen Energy 2010;35:9544–9. https://doi.org/10.1016/j.ijhydene.2010.06.065.

[29] Stoots C, O'Brien J, Hartvigsen J. Results of recent high temperature coelectrolysis studies at the Idaho National Laboratory. Int J Hydrogen Energy 2009;34:4208–15. https://doi.org/10.1016/j.ijhydene.2008.08.029.

[30] Riedel M, Heddrich MP, Friedrich KA. Experimental analysis of the Co-electrolysis operation under pressurized conditions with a 10 layer SOC stack. J Electrochem Soc 2020;167:024504. https://doi.org/10.1149/1945-7111/ab6820.

[31] Tanaka Y, Hoerlein MP, Schiller G. Numerical simulation of steam electrolysis with a solid oxide cell for proper evaluation of cell performances. Int J Hydrogen Energy 2016;41:752–63. https://doi.org/10.1016/j.ijhydene.2015.11.048.

[32] Aicart J, Petitjean M, Laurencin J, Tallobre L, Dessemond L. Accurate predictions of H2O and CO2 co-electrolysis outlet compositions in operation. Int J Hydrogen Energy 2015;40:3134–48. https://doi.org/10.1016/j.ijhydene.2015.01.031.

[33] Zahadat P, Milewski J. Modeling electrical behavior of solid oxide electrolyzer cells by using artificial neural network. Int J Hydrogen Energy 2015;40:7246–51. https://doi.org/10.1016/J.IJHYDENE.2015.04.042.

[34] Kong L, Yu J, Zhu H, Zhu Q, Yan Q. Effect of three parameters of the periodic rectangular pulsed heat flux on the electrical performance improvement to a thermoelectric generator. Energy 2022;261:125175. https://doi.org/10.1016/J.ENERGY.2022.125175.

[35] Tao Y, Ebbesen SD, Mogensen MB. Degradation of solid oxide cells during co-electrolysis of steam and carbon dioxide at high current densities. J Power Sources 2016;328:452–62. https://doi.org/10.1016/j.jpowsour.2016.08.055.

[36] Sun X, Hendriksen PV, Mogensen MB, Chen M. Degradation in solid oxide electrolysis cells during long term testing. Fuel Cell 2019;19:740–7. https://doi.org/10.1002/FUCE.201900081.

[37] Lang M, Raab S, Lemcke MS, Bohn C, Pysik M. Long-Term behavior of a solid oxide electrolyzer (SOEC) stack. Fuel Cell 2020;20:690–700. https://doi.org/10.1002/FUCE.201900245.

[38] Zhang L, Li X, Jiang J, Li S, Yang J, Li J. Dynamic modeling and analysis of a 5-kW solid oxide fuel cell system from the perspectives of cooperative control of thermal safety and high efficiency. Int J Hydrogen Energy 2015;40:456–76. https://doi.org/10.1016/j.ijhydene.2014.10.149.

[39] Skafte TL, Guan Z, Machala ML, Gopal CB, Monti M, Martinez L, et al. Selective high-temperature CO2 electrolysis enabled by oxidized carbon intermediates. Nat Energy 2019;4:846–55. https://doi.org/10.1038/S41560-019-0457-4.

[40] Chen M, Sun X, Hauch A, Brodersen K, Charlas B, Molin S, et al. Final Report for Energinet.dk project no. 2013-1-12013 Solid oxide electrolysis for grid balancing. 2015. https://doi.org/10.13140/RG.2.2.20291.09760.

Please cite this article as: Sánchez-Luján J et al., Optimal integration modeling of Co – Electrolysis in a power-to-liquid industrial process, International Journal of Hydrogen Energy, https://doi.org/10.1016/j.ijhydene.2023.07.012

[41] Wang Y, Banerjee A, Deutschmann O. Dynamic behavior and control strategy study of CO2/H2O co-electrolysis in solid oxide electrolysis cells. J Power Sources 2019;412:255–64. https://doi.org/10.1016/j.jpowsour.2018.11.047.
[42] Suk Kim J, McKellar M, Bragg-Sitton SM, Boardman RD. Status on the component models developed in the modelica framework: high-temperature steam electrolysis plant & gas turbine power plant. 2016. https://doi.org/10.2172/1333156.
[43] Kamkeng ADN, Wang M. Long-term performance prediction of solid oxide electrolysis cell (SOEC) for CO2/H2O co-electrolysis considering structural degradation through modelling and simulation. Chem Eng J 2022;429:132158. https://doi.org/10.1016/J.CEJ.2021.132158.
[44] Dry ME. The fischer–tropsch process: 1950–2000. Catal Today 2002;71:227–41. https://doi.org/10.1016/S0920-5861(01)00453-9.
[45] Pandey U, Runningen A, Gavrilović L, Jørgensen EA, Putta KR, Rout KR, et al. Modeling <scp>Fischer–Tropsch</scp> kinetics and product distribution over a cobalt catalyst. AIChE J 2021;67. https://doi.org/10.1002/aic.17234.
[46] Rytter E, Holmen A. Consorted vinylene mechanism for cobalt fischer–tropsch synthesis encompassing water or hydroxyl assisted CO-activation. Top Catal 2018;61:1024–34. https://doi.org/10.1007/s11244-018-0932-3.
[47] Iglesia E, Reyes SC, Madon RJ, Soled SL. Selectivity control and catalyst design in the fischer-tropsch synthesis: sites, pellets, and reactors. 1993. p. 221–302. https://doi.org/10.1016/S0360-0564(08)60579-9.
[48] Todic B, Ma W, Jacobs G, Davis BH, Bukur DB. CO-insertion mechanism based kinetic model of the Fischer–Tropsch synthesis reaction over Re-promoted Co catalyst. Catal Today 2014;228:32–9. https://doi.org/10.1016/j.cattod.2013.08.008.
[49] van Steen E, Schulz H. Polymerisation kinetics of the Fischer–Tropsch CO hydrogenation using iron and cobalt based catalysts. Appl Catal Gen 1999;186:309–20. https://doi.org/10.1016/S0926–860X(99)00151-9.
[50] Ma W, Jacobs G, Sparks DE, Spicer RL, Davis BH, Klettlinger JLS, et al. Fischer–Tropsch synthesis: kinetics and water effect study over 25%Co/Al2O3 catalysts. Catal Today 2014;228:158–66. https://doi.org/10.1016/j.cattod.2013.10.014.
[51] Brea P, Delgado JA, Águeda VI, Uguina MA. Modeling of breakthrough curves of N2, CH4, CO, CO2 and a SMR type off-gas mixture on a fixed bed of BPL activated carbon. Sep Purif Technol 2017;179:61–71. https://doi.org/10.1016/j.seppur.2017.01.054.
[52] Yang S-I, Choi D-Y, Jang S-C, Kim S-H, Choi D-K. Hydrogen separation by multi-bed pressure swing adsorption of synthesis gas. Adsorption 2008;14:583–90. https://doi.org/10.1007/s10450-008-9133-x.
[53] Li B, He G, Jiang X, Dai Y, Ruan X. Pressure swing adsorption/membrane hybrid processes for hydrogen purification with a high recovery. Front Chem Sci Eng 2016;10:255–64. https://doi.org/10.1007/s11705-016-1567-1.
[54] Grande CA, Blom R. Utilization of dual-PSA technology for natural gas upgrading and integrated CO2 capture. Energy Proc 2012;26:2–14. https://doi.org/10.1016/j.egypro.2012.06.004.
[55] Delgado Dobladez JA, Águeda Maté VI, Torrellas SÁ, Larriba M, Brea P. Efficient recovery of syngas from dry methane reforming product by a dual pressure swing adsorption process. Int J Hydrogen Energy 2021;46:17522–33. https://doi.org/10.1016/j.ijhydene.2020.02.153.
[56] Ma R, Xu B, Zhang X. Catalytic partial oxidation (CPOX) of natural gas and renewable hydrocarbons/oxygenated hydrocarbons—a review. Catal Today 2019;338:18–30. https://doi.org/10.1016/j.cattod.2019.06.025.
[57] Pauletto G, Libretto N, Boffito DC, Miller JT, Jentys A, Patience GS, et al. Ni/CeO2 promoted Ru and Pt supported on FeCrAl gauze for cycling methane catalytic partial oxidation—CPOX. Appl Catal, B 2021;286:119849. https://doi.org/10.1016/J.APCATB.2020.119849.
[58] Arku P, Regmi B, Dutta A. A review of catalytic partial oxidation of fossil fuels and biofuels: recent advances in catalyst development and kinetic modelling. Chem Eng Res Des 2018;136:385–402. https://doi.org/10.1016/J.CHERD.2018.05.044.
[59] Ragauskas AJ, Beckham GT, Biddy MJ, Chandra R, Chen F, Davis MF, et al. Lignin valorization: improving lignin processing in the biorefinery. Science 2014;344. https://doi.org/10.1126/science.1246843. 1979.
[60] Ma R, Guo M, Zhang X. Recent advances in oxidative valorization of lignin. Catal Today 2018;302:50–60. https://doi.org/10.1016/j.cattod.2017.05.101.
[61] Mostafa A, Uysal Y, Junior RBS, Beretta A, Groppi G. Catalytic partial oxidation of ethanol over Rh-coated monoliths investigated by the axially resolved sampling technique: effect of H2O co-feed. Catal Today 2021;367:71–82. https://doi.org/10.1016/J.CATTOD.2020.09.030.
[62] Plazas-González M, Guerrero-Fajardo CA, Sodré JR. Modelling and simulation of hydrotreating of palm oil components to obtain green diesel. J Clean Prod 2018;184:301–8. https://doi.org/10.1016/J.JCLEPRO.2018.02.275.
[63] Cavalcanti CJS, Ravagnani MASS, Stragevitch L, Carvalho FR, Pimentel MF. Simulation of the soybean oil hydrotreating process for green diesel production. Cleaner Chemical Engineering 2022;1:100004. https://doi.org/10.1016/J.CLCE.2022.100004.
[64] Furfari S, Clerici A. Green hydrogen: the crucial performance of electrolysers fed by variable and intermittent renewable electricity. The European Physical Journal Plus 2021;136:509. https://doi.org/10.1140/epjp/s13360-021-01445-5.
[65] Skov IR, Schneider N. Incentive structures for power-to-X and e-fuel pathways for transport in EU and member states. Energy Pol 2022;168:113121. https://doi.org/10.1016/J.ENPOL.2022.113121.

Please cite this article as: Sánchez-Luján J et al., Optimal integration modeling of Co – Electrolysis in a power-to-liquid industrial process, International Journal of Hydrogen Energy, https://doi.org/10.1016/j.ijhydene.2023.07.012